International Journal of Mechanical, Industrial and Aerospace Sciences
ISSN: 2517-9950
Vol:5, No:6, 2011

Vortex-Shedding Suppression in Mixed Convective Flow past a Heated Square Cylinder

A. Rashid and N. Hasan

***Abstract*—**The present study investigates numerically the phenomenon of vortex-shedding and its suppression in two-dimensional mixed convective flow past a square cylinder under the joint influence of buoyancy and free-stream orientation with respect to gravity. The numerical experiments have been conducted at a fixed Reynolds number (Re) of 100 and Prandtl number (Pr) of 0.71, while Richardson number (Ri) is varied from 0 to 1.6 and free-stream orientation, α, is kept in the range $0^o \leq \alpha \leq 90^o$, with 0^o corresponding to an upward flow and 90^o representing a cross-flow scenario, respectively. The continuity, momentum and energy equations, subject to Boussinesq approximation, are discretized using a finite difference method and are solved by a semi-explicit pressure correction scheme. The critical Richardson number, leading to the suppression of the vortex-shedding (Ri_c), is estimated by using Stuart-Landau theory at various free-stream orientations and the neutral curve is obtained in the Ri-α plane. The neutral curve exhibits an interesting non-monotonic behavior with Ri_c first increasing with increasing values of α upto 45^o and then decreasing till 70^o. Beyond 70^o, the neutral curve again exhibits a sharp increasing asymptotic trend with Ri_c approaching very large values as α approaches 90^o. The suppression of vortex shedding is not observed at $\alpha = 90^o$ (cross-flow). In the unsteady flow regime, the Strouhal number (St) increases with the increase in Richardson number.

***Keywords*—**bluff body, buoyancy, free-stream orientation, vortex-shedding.

I. Introduction

FLUID flow past a bluff body experiences separation that produces counter-rotating low-pressure vortices on the downstream side of the bluff body. Depending on the flow parameters, the vortices remain stable leading to a steady flow or are shed periodically from either side of the bluff body leading to a time-periodic flow. The study of bluff body wakes is important from the point of view of applications in aerodynamics, wind engineering, design of long spanned bridges, and towering structures etc. The periodic force loading on the structure, generated due to alternate shedding of vortices, induces structural vibration and noise leading to catastrophic affects.

The methods that are employed for controlling vortex-shedding from bluff bodies can be broadly categorized as, (i) passive and (ii) active control methods. Attaching a splitter plate to the downstream side of the bluff body and streamlining the structures helps in reducing vortex-shedding. Sharp-edged helical strakes are widely used to control the vortex-shedding from chimney stacks, towers, suspended pipes and cables. Introduction of a control cylinder in the wake of a bluff body, to control the phenomenon of vortex-shedding, is another example of passive control approach [1]-[5].

Active control strategies attempt to control vortex-shedding from bluff bodies by generating forces in the flow that alter the flow dynamics. Control via generation of body forces of thermal or electromagnetic origin in the flow, is an example of active control strategy. Rotation and oscillatory motion of bluff bodies represent another type of active control approach for controlling the phenomenon of vortex-shedding. The present study focuses on the control of vortex-shedding by heating the bluff-body. It is well known that the density differences in the fluid caused by thermal effects generate buoyancy forces in the fluid in the presence of an externally imposed body force field like gravity. These buoyancy forces affect the flow dynamics in a complex manner by regulating both (a) particle linear momentum and (b) the particle vorticity (baroclinic effect). It is also known that if the buoyancy effects are sufficiently large in comparison to the fluid inertia, the vortex-shedding can be suppressed [6]-[14], [16], [17].

Most of the earlier studies on mixed convective flow past bluff-bodies have considered either the cross-flow configuration or the configuration in which the buoyancy forces are aligned with the direction of the free-stream (opposing / aiding). Further, either the circular cylinder or the square cylinder has been considered as the representative bluff-body geometry. The case of square cylinder is much more complicated than the circular cylinder owing to the sensitivity of the flow dynamics to the free-stream orientation even in the forced convective flow regime.

The generic problem of two-dimensional mixed convective flow past a heated / cooled square cylinder involving the effects of free-stream orientation and buoyancy together has received very little attention. Fig. 1 depicts a square cylinder kept in a free-stream approaching with a velocity of U_∞ at an orientation specified by the angle 'α'. The temperature difference between the body and the fluid gives rise to buoyancy effect in the presence of gravity force. The buoyancy force would act in positive y-direction, if the temperature of the body is higher than the surrounding fluid and vice-versa. The flow dynamics in the generic scenario is characterized by five dimensionless parameters given as,

A. Rashid is with the Zakir Husain College of Engineering and Technology, Aligarh Muslim University, Aligarh, UP, Pin-202002, INDIA (phone: +91-9450458907; e-mail: rashid_ali10@rediffmail.com).

N. Hasan is with the Zakir Husain College of Engineering and Technology, Aligarh Muslim University, Aligarh, UP, Pin-202002, INDIA (phone: +91-9719517185; e-mail: nadhasan@gmail.com).

i) Reynolds number (Re) = $U_\infty d / \upsilon_0$
ii) Richardson number (Ri) = $(g\beta(T_s - T_\infty)d) / U_\infty^2$
iii) Prandtl number (Pr) = υ_0 / κ_0
iv) Free stream orientation with respect to gravity = α
v) Cylinder orientation with respect to the x-axis = ϕ

It is worth mentioning that for the forced flow, α and ϕ, cease to act as independent parameters and rather any one of them can be used to fix the cylinder orientation with respect to the free-stream. In the above dimensionless numbers, 'U_∞' is the free stream velocity, 'd' is the characteristic length scale of the body, 'g' is the gravitational intensity, 'β' is the coefficient of volume expansion, 'T_s' is the uniform cylinder temperature, 'T_∞' is the free-stream fluid temperature, υ_0 and κ_0 are the kinematic viscosity and thermal diffusivity at some reference temperature T_0 which is chosen to be the free stream fluid temperature T_∞.

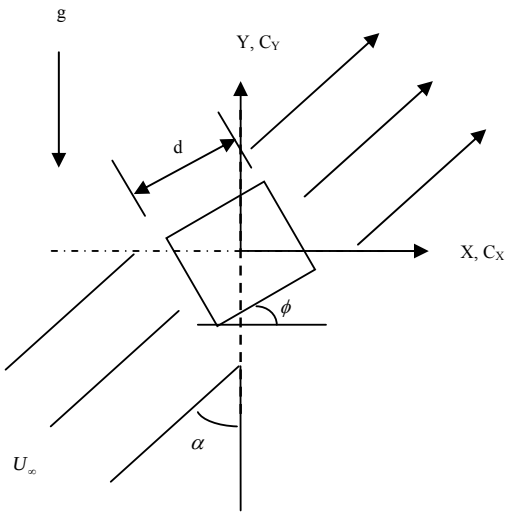

Fig. 1 Definition of the geometry and integration domain of two-dimensional flow past a square cylinder

The phenomenon of vortex-shedding (and its suppression) for two-dimensional mixed convective flows has been studied mostly in the context of square and circular cylinders. Sharma and Eswaran [13] studied numerically the two-dimensional mixed convective flow and heat transfer characteristics around a square cylinder maintained at a constant temperature for α = 0°. They considered the effect of heating (Ri > 0, aiding buoyancy) as well as cooling (Ri < 0, opposing buoyancy) with the values of Ri varied in the range (-1, 1) at (Re = 100, Pr = 0.7, ϕ = 0°). The vortex-shedding suppression or the disappearance of the Karman vortex street was found to occur at a critical Richardson number of 0.15.

Sharma and Eswaran [14] studied the effect of channel-confinement of various degree (blockage ratio of 10%, 30%, and 50%) on the two-dimensional upward flow (α = 0°) and heat transfer characteristics around a heated/cooled square cylinder by considering the aiding/opposing buoyancy by varying the values of Ri in the range (-1, 1) at (Re = 100, Pr = 0.7 and ϕ = 0°). It was shown that with increasing blockage ratio, the minimum heating (critical Ri) required for the suppression of vortex-shedding decreases up to a certain blockage ratio (= 30%), but thereafter increases. At a constant blockage ratio (= 30%), the value of Ri at which vortex-shedding is suppressed increases with Re.

Bhattacharyya and Mahapatra [15] studied numerically the influence of buoyancy on vortex shedding and heat transfer from a two-dimensional square cylinder exposed to a horizontal stream (α = 90°, ϕ = 0°) for (100 ≤ Re ≤1400, 0 ≤ Ri ≤ 1) at Prandtl number of 0.72. They found that the centerline symmetry of the wake was lost and the cylinder experiences a mean downward lift when the buoyancy effect was considered. Vortex-shedding suppression was not observed for any value of Ri.

Singh et al. [16] investigated experimentally the wakes behind heated circular and square cylinders by schlieren-interferometry for (α = 0°, ϕ = 0°). The disappearance of vortex-shedding was observed at Ri = 0.122 for Re = 94 and at Ri = 0.157 for Re = 110 for a circular cylinder. The critical Ri values for a square cylinder were reported equal to 0.107, 0.121, 0.140, 0.155, and 0.171 for Re = 87, 94, 103, 109, and 118, respectively.

Kakade et al. [17] studied experimentally the joint influence of buoyancy and orientation of a square cylinder (ϕ) on vortex-shedding and wake characteristics at α = 0° for (Re = 56, 87, and 100, Ri = 0.031-0.291 and 0 ≤ ϕ ≤ 45°). They showed that at a Reynolds number of 56 and an incidence angle of 0°, vortex-shedding was absent at all Richardson numbers. At Reynolds numbers of 87 and 100 and Ri ≠ 0, regular vortex-shedding was observed for all incidence angles. However at higher Richardson numbers, vortex-shedding was suppressed.

The present study reports the phenomenon of vortex-shedding suppression past a square cylinder in two-dimensional mixed convective laminar flow regime, under the joint influence of buoyancy and free-stream orientations (α) with respect to gravity. The numerical experiments have been conducted at Re = 100, Pr = 0.71 and ϕ = 0°. The free-stream orientations and Ri are varied in the ranges of 0° ≤ α ≤ 90° and 0 ≤ Ri ≤ 1.6. At each value of α, a series of computations are carried out in the unsteady flow regime near the critical point (vortex-shedding suppression point) and the equilibrium amplitudes of oscillations of the periodic flow are utilized to estimate the critical values of the Richardson number Ri by employing the Stuart-Landau theory. In this manner, neutral curve in the (Ri- α) plane, separating the steady and unsteady flow regimes is obtained. In the unsteady flow regime, the shedding frequency or the Strouhal number is estimated for different combinations of Ri and α.

II. Mathematical Formulation

In the present study the flow field is taken to be two-dimensional, unsteady, viscous and laminar. The effects of buoyancy are accounted via the Boussinesq approximation (Tritton [18]). Generalized curvilinear (body-fitted) coordinates are employed. The governing equations of mass, momentum and energy in non-dimensional form, subjected to Boussinesq approximation in Cartesian coordinates transformed into body fitted coordinates (Warsi et al. [19]) are given as follows,

Continuity:

$$\left(\frac{y_\eta}{J}\frac{\partial}{\partial\xi}-\frac{y_\xi}{J}\frac{\partial}{\partial\eta}\right)u+\left(-\frac{x_\eta}{J}\frac{\partial}{\partial\xi}+\frac{x_\xi}{J}\frac{\partial}{\partial\eta}\right)v=0 \tag{1}$$

x – Momentum:

$$\frac{\partial u}{\partial\tau}+U^\xi\frac{\partial u}{\partial\xi}+U^\eta\frac{\partial u}{\partial\eta}=-\left(\frac{y_\eta}{J}\frac{\partial\overline{p}}{\partial\xi}-\frac{y_\xi}{J}\frac{\partial\overline{p}}{\partial\eta}\right)+\frac{1}{\mathrm{Re}}\left(A\frac{\partial^2u}{\partial\xi^2}-2B\frac{\partial^2u}{\partial\xi\partial\eta}+C\frac{\partial^2u}{\partial\eta^2}+\tilde{P}\frac{\partial u}{\partial\xi}+\tilde{Q}\frac{\partial u}{\partial\eta}\right) \tag{2}$$

y – Momentum:

$$\frac{\partial v}{\partial\tau}+U^\xi\frac{\partial v}{\partial\xi}+U^\eta\frac{\partial v}{\partial\eta}=-\left(-\frac{x_\eta}{J}\frac{\partial\overline{p}}{\partial\xi}+\frac{x_\xi}{J}\frac{\partial\overline{p}}{\partial\eta}\right)+\frac{1}{\mathrm{Re}}\left(A\frac{\partial^2v}{\partial\xi^2}-2B\frac{\partial^2v}{\partial\xi\partial\eta}+C\frac{\partial^2v}{\partial\eta^2}+\tilde{P}\frac{\partial v}{\partial\xi}+\tilde{Q}\frac{\partial v}{\partial\eta}\right)+Ri\theta \tag{3}$$

Energy Equation:

$$\frac{\partial\theta}{\partial\tau}+U^\xi\frac{\partial\theta}{\partial\xi}+U^\eta\frac{\partial\theta}{\partial\eta}=\frac{1}{\mathrm{Re}\,\mathrm{Pr}}.\left(A\frac{\partial^2\theta}{\partial\xi^2}-2B\frac{\partial^2\theta}{\partial\xi\partial\eta}+C\frac{\partial^2\theta}{\partial\eta^2}+\tilde{P}\frac{\partial\theta}{\partial\xi}+\tilde{Q}\frac{\partial\theta}{\partial\eta}\right) \tag{4}$$

In the above equations, U^ξ and U^η are the dimensionless velocities in ξ and η directions, defined as,

$$U^\xi=\left(\frac{y_\eta}{J}\right)u-\left(\frac{x_\eta}{J}\right)v,\ U^\eta=-\left(\frac{y_\xi}{J}\right)u+\left(\frac{x_\xi}{J}\right)v. \tag{5}$$

The terms A, B, C and J are defined as,

$$A=\left(\frac{y_\eta^2+x_\eta^2}{J^2}\right),\ B=\left(\frac{x_\xi x_\eta+y_\xi y_\eta}{J^2}\right),\ C=\left(\frac{y_\xi^2+x_\xi^2}{J^2}\right),\text{ and}$$

$$J=\left(x_\xi y_\eta-x_\eta y_\xi\right) \tag{6}$$

In order to convert the basic equations to non-dimensional form, the following scales are selected:

i) Length scale = edge of square cylinder ≡ 'd'.
ii) Velocity scale = free-stream speed ≡ 'U_∞'.
iii) Time scale ='d/U_∞'.

The changes in fluid temperature and pressure scale as (T_s-T_∞) and $\rho_0U_\infty^2$ respectively, and the dimensionless temperature and pressure are accordingly defined as,

$$\theta=\frac{T-T_\infty}{T_s-T_\infty},\quad \overline{p}=\frac{p-p_\infty}{\rho_0U_\infty^2} \tag{7}$$

The extra diffusion terms in (2)-(4) involving $\tilde{P}$ and $\tilde{Q}$ arises due to the transformation of the laplacian diffusion term into generalized curvilinear coordinates (Warsi et al. [19]). These terms are related to the transformation metrics as,

$$\nabla^2\xi=\tilde{P},\ \nabla^2\eta=\tilde{Q} \tag{8}$$

III. Numerical Details

In this section the grid structure, numerical scheme and boundary conditions are presented.

A. Grid Structure

Elliptic grid generation technique is used to develop an O-type grid. Elliptic grid generation is one of the several methods used to generate structured grids for odd geometries. The simplest elliptic grid is the one governed by the Laplace's equation i.e.

$$\nabla^2\xi=0,\quad \nabla^2\eta=0 \tag{9}$$

In order to generate the grid, the infinite physical domain is truncated by an artificial boundary. The geometry of the artificial boundary surrounding the cylinder is taken to be a concentric circle of a diameter that is large compared to that of the cylinder. The truncated physical x-y domain is then mapped on the rectangular domain in the ξ-η computational plane using well established techniques [19].

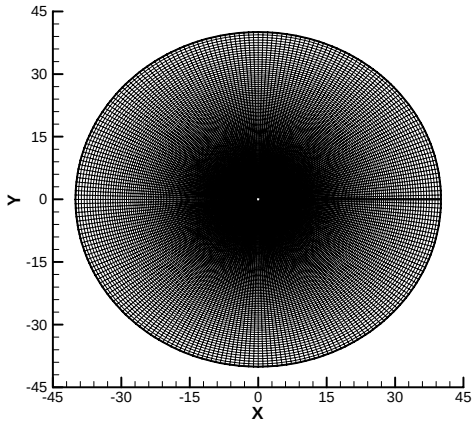

Fig. 2(a) Structured Grid (241x325) in physical x-y plane

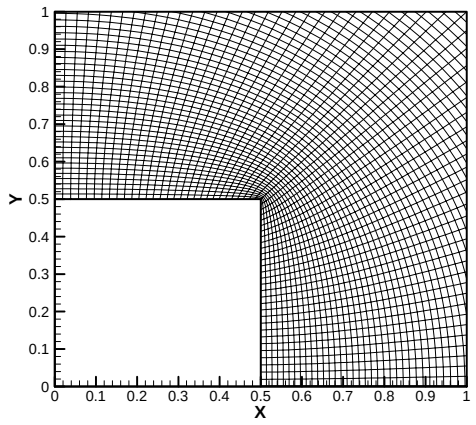

Fig. 2(b) Magnified view of grid near the cylinder surface

Equations (9) are inverted and discretized on a uniform grid in the computational plane to obtain the grid in the physical plane. Therefore, for the laplacian grids employed, the terms $\tilde{P}$ and $\tilde{Q}$, according to (8), are taken to be zero in (2)-(4).

Fig. 2 (a) shows the typical structured grid of 241x325 and Fig. 2 (b) the magnified view of the grid near the cylinder surface.

B. Numerical Scheme

The governing equations are discretized on a colocated, non-staggered body fitted grid by employing finite difference type of spatial discretization. A semi-explicit, pressure correction scheme [20], [21] is employed for advancing the discrete solution in time from a given set of initial conditions. The diffusion terms were treated explicitly in [20], [21], however in the present study the diffusion terms are treated implicitly in the predictor step of pressure correction scheme, permitting the use of much larger time steps than permitting by a fully explicit treatment. The concept of momentum interpolation of Rhie and Chow [22] is utilized in order to avoid grid scale pressure oscillations that can result, owing to the decoupling of the velocity and pressure at a grid point in a colocated arrangement. The scheme is conceptually similar to the SMAC algorithm [23]-[25].

C. Boundary and Initial Condition

At the surface of the cylinder the no-slip and no penetration condition is applied for velocity components. The cylinder is taken to be at a uniform but elevated temperature T_s. Mathematically, these conditions in non dimensional form are expressed as,

$$u = v = 0\,,\ \theta = 1.0\,. \tag{10}$$

At infinitely large distance from the cylinder the free-stream condition exists. Mathematically,

$$\vec{V} = \vec{U} = \left(c\cos\alpha\,\hat{i} + sin\alpha\,\hat{j}\right),\ \theta = 0 \tag{11}$$

The conditions specified in (11) cannot be employed on the entire artificial boundary at relatively short distances. Therefore numerical boundary conditions must be employed at the artificial boundary. In order to apply the numerical boundary conditions, the artificial boundary is divided into two halves, i) the inflow portion and ii) the outflow portion on the basis of the direction of the local normal velocity.

At the inflow portion, the velocity and temperature are specified as in (11). For pressure the normal momentum equation is employed.

At the outflow portion, for velocities, the proposed numerical boundary conditions at the outflow portion by Hasan et al. [21] are employed. These conditions permit the placement of artificial boundary at relatively short distances from the body without significantly affecting the flow dynamics. For temperature a convective boundary condition (Orlanski [26]) is applied which is given as,

$$\frac{\partial\theta}{\partial\tau} + U_c\frac{\partial\theta}{\partial\eta} = 0\,, \tag{12}$$

where, U_c is the local normal fluid velocity.

For pressure the traction-free boundary condition (Gresho [27]), Cheng and Armfield [25]) is utilized. It is given as,

$$p = \frac{1}{\mathrm{Re}}\frac{\partial U^n}{\partial n}\,. \tag{13}$$

In the above equation n is the local normal and U^n is the local normal velocity.

IV. Numerical Aspects and Validation Studies

In this section the effects of grid size, time step, location of artificial boundary, are presented to demonstrate the sensitivity of the computations on these numerical aspects. Further, the accuracy of the computed data is demonstrated with the help of validation exercises in which the global parameters like drag, Nusselt number are compared with the data available in literature. From the application point of view, the effect of flow past bluff body is perceived in terms of gross quantities like forces exerted by the fluid on the object and the total heat transfer rate between the body and the fluid. For the two dimensional problem considered, the gross quantities are, Lift or transverse force, Drag or stream wise force and Total heat transfer rate. In a non-dimensional framework, these gross quantities are expressed in a dimensionless manner as follows,

i) Lift coefficient, $(C_L) = C_Y \sin\alpha - C_x \cos\alpha$

ii) Drag coefficient, $(C_D) = C_X sin\alpha + C_Y cos\alpha$

iii) Nusselt number, $(Nu) = Q/(4k(T_s - T_\infty))$

Where, $C_X = (2F_X)/(\rho U_\infty^2 bd), C_Y = (2F_Y)/(\rho U_\infty^2 bd)$

In the above equations F_X, F_Y and Q are the stream wise force, transverse force and heat transfer. The quantity Q is expressed on a unit span basis of the cylinder.

A. Grid Size and time step

The effect of grid size is studied for the forced flow regime by fixing the far boundary at a distance of 40d from the center of the cylinder at (Re = 100, Pr = 0.71, $\alpha = 0^o$, $\phi = 0^o$) and a time step of 0.001 dimensionless units. Three grids having 161×225 (G1), 241×325 (G2) and 321×425 (G3) mesh points are employed. In going from grid G1 to G2 the change in the flow parameters like mean drag coefficient and Strouhal number is less than 1%. This indicates that the % change in the flow parameters is very small in going from G1 to G2 or G2 to G3, therefore the grid size of 241×325 is considered suitable for grid-independent computations.

For the study of influence of time step, the computations are also performed at time step of 0.0005 dimensionless units for (Re = 100, Pr = 0.71, Ri = 0, $\alpha = 0^o$, $\phi = 0^o$). The percentage change in mean drag coefficient is 0.027 when going from time step of 0.0005 to 0.001. It is concluded from the above discussion that the smaller time step had no significant effect on the results therefore the time step of 0.001 dimensionless units is chosen for the entire computations.

B. Location of Artificial Boundary

An exercise is carried out to determine a suitable position for the artificial boundary, such that the numerical boundary conditions imposed on it do not significantly influence the flow dynamics in the vicinity of the square cylinder. Initially the distance of the far boundary is fixed at 120 dimensionless units form the center of the cylinder and a grid is generated. Then the grid is truncated at distances of 100, 80, 60, 40 and 20 dimensionless units to yield progressively smaller domain with identical grid sizes in the ξ and η directions. For each choice of the location of the far boundary, computation is performed for Re = 100, Pr = 0.71, Ri = 0, $\alpha = 0^o$, $\phi = 0^o$ and the lift and drag coefficients and Strouhal number are calculated. For distance beyond 20, the changes in the values of mean lift coefficient, mean drag coefficient and Strouhal number are quite small. Therefore, a distance in excess of 20 is considered suitable for computations. For the entire computations the artificial boundary is located at a distance of 40 dimensionless units.

C. Validation

The forced flow past a fixed square cylinder ($\phi = 0^o$) is considered for the conditions, Re = 100, Pr = 0.71 and free-stream orientations 0-45^o. The variation of mean coefficient of drag and the mean Nusselt number with free-stream orientation is obtained and compared with the available data of Sohankar et al. [28] and Ranjan et al. [29] as shown in Figs. 3(a)-3(b). The present results of drag coefficient are in good agreement with Sohankar et al. [28] and also in agreement with Ranjan et al. [29]. The computed mean Nusselt number is in good agreement with Ranjan et al. [29].

The computations are also carried out for fixed stationary square cylinder ($\phi = 0^o$) for the conditions, Re = 100, Pr = 0.71, $\alpha = 0^o$ and $0 \leq Ri \leq 1.2$ in the mixed convection flow regime. The variation of mean coefficient of drag and mean Nusselt number with Richardson number is computed and compared with the available data of Sharma and Eswaran [13] in Figs. 4(a)-4(b).

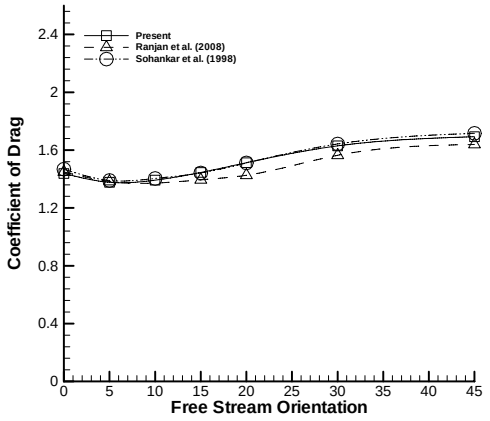

Fig. 3(a) Variation of coefficient of drag with free-stream orientation

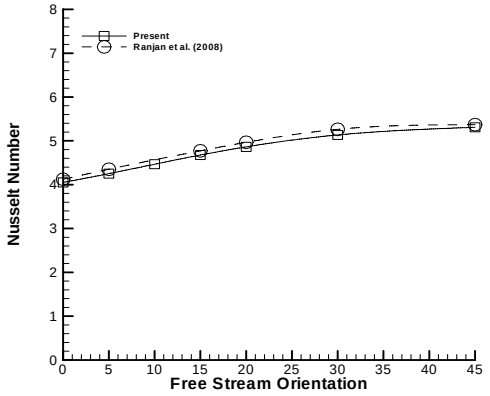

Fig. 3(b) Variation of mean Nusselt number with free-stream orientation

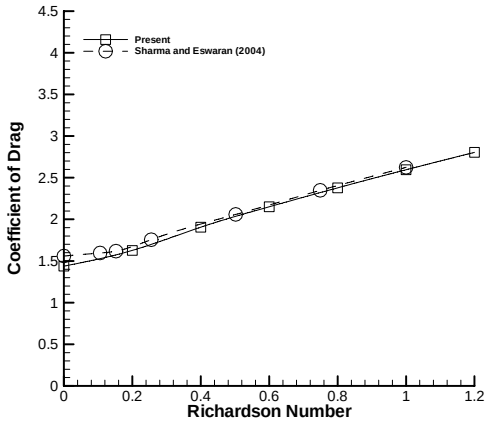

Fig. 4(a) Variation of coefficient of drag with Richardson number

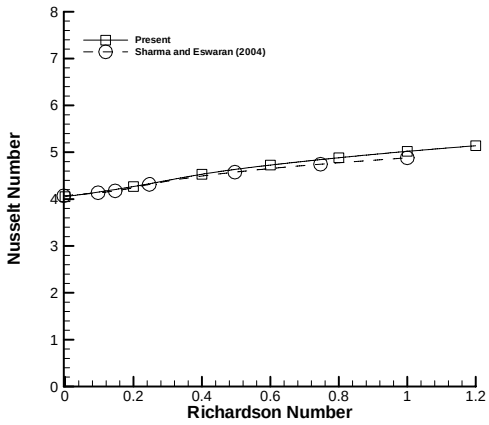

Fig. 4(b) Variation of mean Nusselt number with Richardson number

The present computations are in good agreement with the numerical results of Sharma and Eswaran [13].

V. Results And Discussion

To investigate the vortex-shedding suppression phenomenon, simulations are performed for a set of Richardson numbers close to the vortex-shedding suppression point in the unsteady flow regime at a fixed free-stream orientation. The objective of this exercise is to investigate the character of the bifurcation associated with the vortex-shedding suppression and to determine the critical Richardson number at different free stream orientations. All the computations reported in this section are carried out for a fixed cylinder orientation of ϕ = 0° and at (Re = 100, Pr =0.71).

A. Phenomenon of Vortex-Shedding Suppression

The vortex-shedding for a flow past a stationary cylinder is the outcome of growth of linear unstable mode or perturbation that evolves in time in an oscillatory manner and the scenario is a classical supercritical Hopf bifurcation. After the initial exponential growth in time, the infinitesimal unstable perturbation becomes finite and the non-linear self-interactions alter the exponential growth rate. This scenario was first proposed by Landau (Drazin and Reid, [30]). The growth of the amplitude of the oscillatory unstable mode in time, for small amplitudes, is governed by the famous Landau equation given as,

$$\frac{d}{d\tau}\left(A^2\right) = 2\sigma A^2 - lA^4 . \qquad (14)$$

The constant 'σ' represents the initial exponential growth rate of the amplitude and 'l' is the Landau constant. The steady state amplitude of the unstable mode is readily obtained from (14) by setting $\frac{d}{d\tau}\left(A^2\right) = 0$ as,

$$A_e^2 = \frac{2\sigma}{l} . \qquad (15)$$

Near the critical point, the LHS of (15) can be linearized in terms of some control parameter which, in the present context, is the Richardson number or Ri. Thus by generating straight line fit to the ($A_e^2 - Ri$) data obtained near the critical point or vortex-shedding suppression point, the critical Richardson number, Ri_c, can be readily obtained.

As a quantitative confirmation of the above arguments, the square of the equilibrium oscillatory flow amplitude obtained from the time history of lift coefficient is plotted as a function of the control parameter Ri in Fig. 5 for $\alpha = 0^o$.

The data agrees well with a straight line fit having a negative slope. This confirms that the vortex-shedding and its suppression in the context of the present problem is a supercritical Hopf bifurcation. The negative slope clearly implies that the exponential growth rate of the linearly unstable mode, σ, changes sign from positive to negative with increase in Ri across the critical point leading to suppression of the vortex-shedding. Extrapolating the straight line fit, the critical Richardson number (Ri_c) is estimated to be 0.129 at Re = 100 and free-stream orientation $\alpha = 0^o$. The numerical and experimental values of critical Richardson (Ri_c) number reported by Turki et al. [31] and Kakade et al. [17] are 0.130 and 0.131 under the same conditions, and are in excellent agreement with the present estimate.

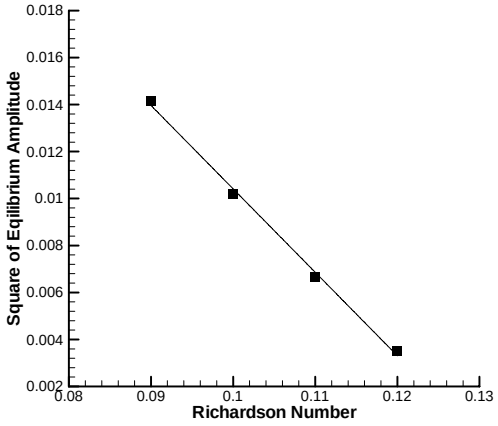

Fig. 5 Variation of square of equilibrium amplitudes with the control parameter Ri in the neighbourhood of suppression or bifurcation for Re = 100, Pr = 0.71 and free-stream orientation (α) of 0°

By carrying out the above exercise for different free-stream orientations in the range of $0^o \leq \alpha < 90^o$, the straight line fits for the $A_e^2 - Ri$ data have been obtained and the critical Ri determined. At $\alpha = 90^o$, vortex-shedding suppression is not observed within the range of Ri considered in the present study.

Fig. 6 shows an interesting non-monotonic neutral curve in the Ri-α plane demarcating the steady and the unsteady flow regimes. The critical Ri increases rapidly with increase in α upto 45°, beyond which it again drops till about 70°. Further,

increase in α leads to a very sharp almost asymptotic increase in the critical Richardson number.

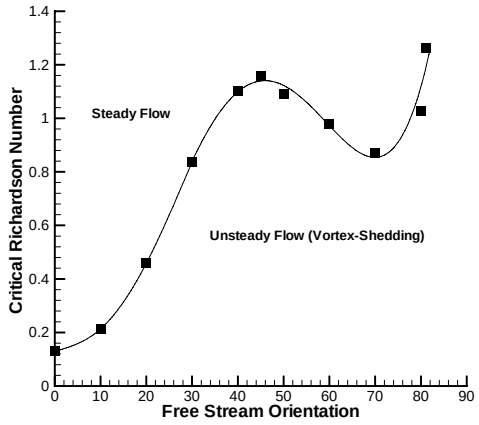

Fig. 6 Variation of critical Richardson number with free-stream orientation

A detailed investigation of the wake is required to comprehend the possible reason for such an interesting suppression characteristic.

B. Strouhal Number in the unsteady flow regime

The Strouhal number (St) represents the characteristic dimensionless frequency of vortex-shedding from the square cylinder and therefore represents a fundamental property associated with the observed periodic flow. The time history of coefficient of lift is employed to obtain the dimensionless frequencies or the Strouhal numbers. The effect of free-stream orientation for the forced flow on St is depicted in Fig. 7. As shown in Fig. 7, the Strouhal number shows a very slight sensitivity to free-stream orientation for the forced flow. It decreases by only 5% at $\alpha = 45^o$ relative to the value observed at $\alpha = 0^o$.

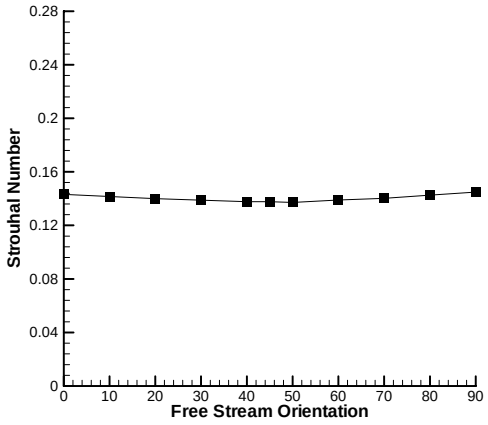

Fig. 7 Variation of Strouhal number with free-stream orientation

In the mixed convective flow regime, the variation of Strouhal number with Richardson number at various free-stream orientations is shown in Figs. 8(a)-8(g). In order to highlight the effect of buoyancy, the values of St for a given free-stream orientation are normalized by the corresponding forced flow value. It is seen from the figure that the Strouhal number increases smoothly with the increase in Richardson number and suddenly falls to zero beyond the critical Richardson number. The trend remains the same for all free-stream orientations except for the case of $\alpha = 90^o$, where the phenomenon of vortex shedding suppression does not occur. Bhattacharyya and Mahapatra [15] also reported that the vortex-shedding suppression did not occur when the cylinder was exposed to a horizontal cross flow.

Increase in St with Ri can be qualitatively explained in the following manner. As the shear layers surrounding the separated flow region or vortices gain momentum under the influence of buoyancy, the residence time is decreased in the shear layers leading to lesser transfer of momentum and vorticity in the separated flow. This reduces the ability of the vortex or separated zone to resist the instability responsible for vortex-shedding. Therefore, vortices do not remain stable for longer time intervals and instead are shed more frequently. The effect is essentially same as obtained by increasing the Reynolds number of the flow.

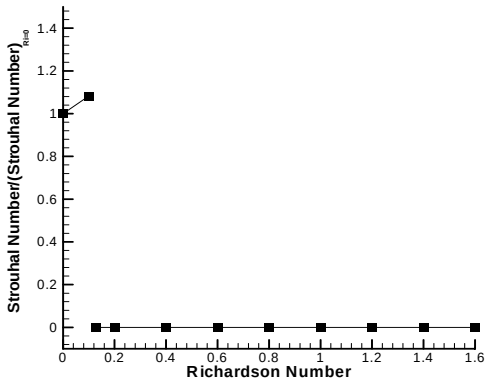

(a)

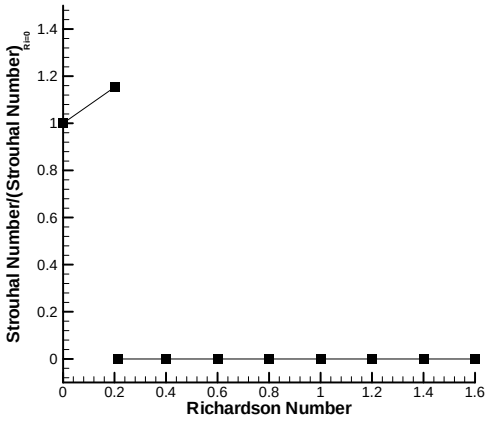

(b)

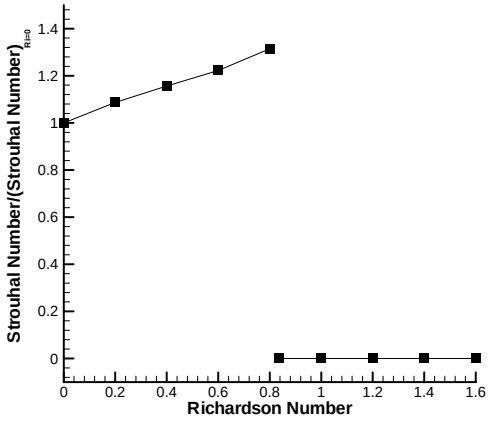

(c)

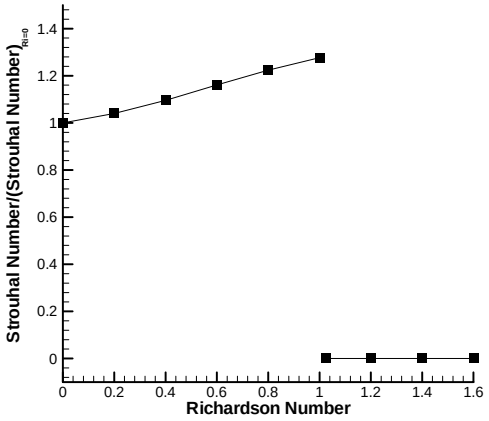

(f)

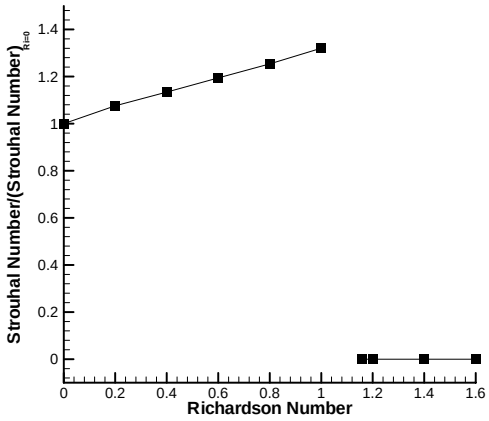

(d)

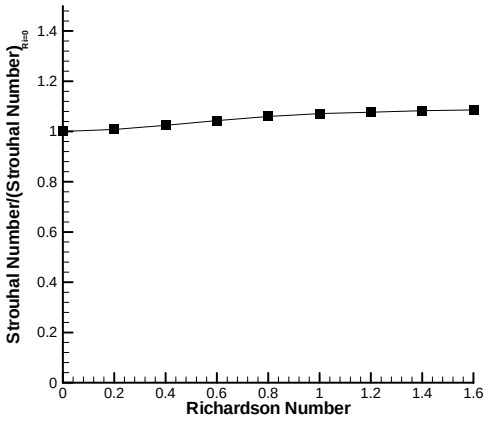

(g)

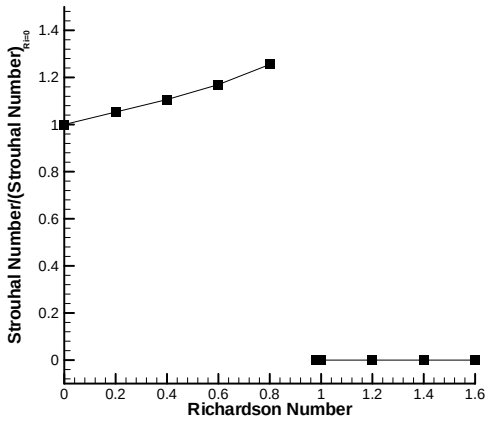

(e)

Fig. 8 Variation of Strouhal number with Richardson number at (a) α = 0°, (b) 10°, (c) 30°, (d) 45°, (e) 60°, (f) 80°, (g) 90°

These arguments are further supported by the observation that increase in free-stream orientation leads to lower sensitivity of Strouhal number to Ri in the unsteady flow regime. This is because at larger free-stream orientations, owing to greater misalignment between fluid inertia and buoyancy forces, buoyancy becomes less effective in imparting acceleration to the shear layers on either side of the separated flow region.

VI. Conclusion

The effect of buoyancy and free-stream orientation on vortex-shedding and its suppression are investigated numerically around a heated square cylinder in the mixed convective flow regime. The highlight of the work is the segregation of the unsteady and the steady flow regimes in the (Ri - α) plane by estimation of the critical Richardson number at different free-stream orientations using the Stuart-landau

theory. To the best of knowledge of the authors such a regime map for the two-dimensional mixed convective flow past a square cylinder has been presented for the first time. The neutral curve in the regime map is an interesting non-monotonic trend that warrants further investigation. The flow is found to be steady when the Richardson number crosses the critical value of 0.129, 0.213, 0.458, 0.837, 1.103, 1.158, 1.089, 0.980, 0.872, 1.027 and 1.262 respectively at free stream orientation of 0^o, 10^o, 20^o, 30^o, 40^o, 45^o, 50^o, 60^o, 70^o, 80^o and 81^o respectively. The flow is always found to be unsteady for cross flow. In the unsteady flow regime, the Strouhal number exhibits a strong sensitivity to Ri with values increasing with increase in Ri. However, the sensitivity is found to decrease with increase in free-stream orientation. These effects have been qualitatively explained on the basis of shear layer momentum gain and transfer to the engulfed separated flow zone or vortices.

REFERENCES

[1] J. H. Gerrard, "The mechanism of the formation region of vortices behind bluff bodies", Journal of fluid mechanics, vol. 25, part 2, 1966, pp 401-413.
[2] E. A. Anderson and A. A. Szewczyk, "Effects of a splitter plate on the near wake of a circular cylinder in 2 and 3-dimensional flow configurations". Experiments in Fluids 23, 1997, pp 161-174.
[3] S. Mittal, "Effect of a ''slip'' splitter plate on vortex shedding from a cylinder", Physics of fluids vol. 15, No. 3, 2003, pp 817-820.
[4] S. E. Razavi, V. Farhangmehe and F. Barar, "Impact of a splitter plate on flow and heat transfer around circular cylinder at low Reynolds numbers", Journal of applied sciences 8(7), 2008, pp 1286-1292.
[5] R. A. Kumar, C-H Sohn and B. H. L. Gowda, "Passive Control of Vortex-Induced Vibrations: An Overview", Recent patents on mechanical engineering, vol. 1, No. 1, Bentham Science Publishers Ltd., 2008, pp 1-11.
[6] Z. Chen and N. Aubry, "Active control of cylinder wake", Communications in nonlinear science and numerical simulation 10, 2005, pp 205–216.
[7] L. Cheng, Y. Zhou and M. M. Zhang, "Controlled vortex-induced vibration on a fix-supported flexible cylinder in cross-flow", Journal of sound and vibration 292, 2005, pp 279-299.
[8] J. Seidel, S. Siegel, C. Fagley, K. Cohen and T. McLaughlin, "Feedback control of a circular cylinder wake", Proc. IMechE Vol. 223 Part G: J. Aerospace Engineering, 2008, pp 379-392.
[9] M. Coutanceau and C. Menard, "Influence of rotation on the near wake development behind an impulsive started circular cylinder", J. fluid mech., 158, 1985, pp 399-446.
[10] S. Mittal, "Control of flow past bluff bodies using rotating control cylinders", Journal of fluids and structures 15, 2001, pp 291-326.
[11] D. Stojkovic, M. Breuer and F. Durst, "Effect of high rotation rates on the laminar flow around a circular cylinder", Physics of fluids vol. 14 No. 9, 2002, pp 3160-3178.
[12] S. Mittal and B. Kumar, "Flow past a rotating cylinder", J. fluid mech. Vol. 476, 2003, pp 303-344.
[13] A. Sharma and V. Eswaran, "Effect of aiding and opposing buoyancy on the heat and fluid flow across a square cylinder at Re = 100", Numerical heat transfer, part A, 45, 2004, pp 601-624.
[14] A. Sharma and V. Eswaran, "Effect of channel-confinement and aiding/opposing buoyancy on the two-dimensional laminar flow and heat transfer across a square cylinder", International journal of heat and mass transfer 48, 2005, pp 5310-5322.
[15] S. Bhattacharyya and S. Mahapatra, "Vortex shedding around a heated square cylinder under the influence of buoyancy", Heat mass transfer 41, 2005, pp 824-833.
[16] S. K. Singh, P. K. Panigrahi and K. Muralidhar, "Effect of buoyancy on the wakes of circular and square cylinders: a schlieren-interferometric study", Exp. fluids 43, 2007, pp 101-123.
[17] A. A. Kakade, S. K. Singh, P. K. Panigrahi and K. Muralidhar, "Schlieren investigation of the square cylinder wake: joint influence of buoyancy and orientation", Physics of fluids 22, 054107, 2010, pp 1-18.
[18] D.J. Tritton, "Physical fluid dynamics", ELBS edition chapter 13, 1979, pp 127-130.
[19] Z. U. A. Warsi, J. F. Thompson and C. M. Mastin, "Numerical Grid Generation", 1984.
[20] N. Hasan and S. Sanghi, "The dynamics of two-dimensional buoyancy driven convection in a horizontal rotating cylinder", Journal of heat transfer, vol. 126, 2004, pp 963-984.
[21] N. Hasan, S. F. Anwer and S. Sanghi, "On the outflow boundary condition for external incompressible flows: A new approach", Journal of computational physics 206, 2005, pp 661-683.
[22] C. M. Rhie and W. L. Chow, "Numerical study of the turbulent flow past an airfoil with trailing edge separation", AIAA J. vol. 21, issue 11, 1983, pp 1525-1532.
[23] A. A. Amsden and F. H. Harlow, "The SMAC method: A numerical technique for calculating incompressible fluid flows", Los Alamos scientific report, LA 4370, 1970.
[24] S. W. Kim and T. J. Benson, "Comparison of the SMAC, PISO and iterative time advancing schemes for unsteady flows", Computers and fluids, vol. 21, issue 3, 1992, pp 435-454.
[25] L. Cheng and S. Armfield, "A simplified marker and cell method for unsteady flows on non-staggered grids", International journal for numerical methods in fluids, Vol. 21, issue 1, 1995, pp 15-34.
[26] I. Orlanski, "A simple boundary condition for unbounded hyperbolic flows", Journal of computational physics vol. 21, 1976, pp 251-269.
[27] P. M. Gresho, "Incompressible fluid dynamics: some fundamental formulation issues", Annual review of fluid mechanics, vol. 23, 1991, pp 413-453.
[28] A. Sohankar, C. Norberg and L. Davidson, "Low-Reynolds-number flow around a cylinder at incidence: study of blockage, onset of vortex shedding and outlet boundary condition", International journal for numerical methods in fluids, vol. 26, 1998, pp 39-56.
[29] R. Ranjan, A. Dalal and G. Biswas, "A numerical study of fluid flow and heat transfer around a square cylinder at incidence using unstructured grids", Numerical heat transfer, part A, 54, 2008, pp 890-913.
[30] P. G. Drazin and W. H. Reid, "Hydrodynamic stability", Cambridge university press, chapter 7, 1981, pp 370-375.
[31] S. Turki, H. Abbassi, S. B. Nasrallah, "Two-dimensional laminar fluid flow and heat transfer in a channel with a built-in heated square cylinder", International journal of thermal sciences 42, 2003, pp 1105-1113.